HHS Public Access

Author manuscript

J Magn Reson Imaging. Author manuscript; available in PMC 2019 June 01.

Published in final edited form as:

J Magn Reson Imaging. 2018 June ; 47(6): 1692–1700. doi:10.1002/jmri.25897.

Feasibility analysis of early temporal kinetics as a surrogate marker for breast tumor type, grade and aggressiveness

Laura Heacock, MD[1], **Alana A. Lewin, MD**[1], **Yiming Gao, MD**[1], **James S. Babb, PhD**[1], **Samantha L. Heller, PhD, MD**[1], **Amy N. Melsaether, MD**[1,2], **Neeti Bagadiya, MD**[1], **Sungheon G. Kim, PhD**[1,2], and **Linda Moy, MD**[1,2]

[1]Bernard and Irene Schwartz Center for Biomedical Imaging, Department of Radiology, New York University School of Medicine, New York, New York, 10016, United States

[2]Center for Advanced Imaging Innovation and Research (CAI[2]R), New York University School of Medicine, New York, New York, 10016, United States

Abstract

Background—Screening breast MRI has been shown to preferentially detect high grade ductal carcinoma in situ (DCIS) and invasive carcinoma, likely due to increased angiogenesis resulting in early initial uptake of contrast. As interest grows in abbreviated screening breast MRI (AB-MRI), markers of early contrast wash-in that can predict tumor grade and potential aggressiveness are of clinical interest.

Purpose—To evaluate the feasibility of using the initial enhancement ratio (IER) as a surrogate marker for tumor grade, hormone receptor status, and prognostic markers, as an initial step to being incorporated into AB-MRI.

Study Type—Retrospective.

Subjects—162 women (mean 55.0 years, range 32.8–87.7 years) with 187 malignancies imaged January 2012–November 2015.

Field Strength/Sequence—Images were acquired at 3.0T with a T1-weighted gradient echo fat suppressed volume interpolated breath-hold sequence.

Assessment—Subjects underwent dynamic contrast-enhanced breast MRI with a 7-channel breast coil. IER (% signal increase over baseline at the first post-contrast acquisition) was assessed and correlated with background parenchymal enhancement, washout curves, stage and final pathology.

Statistical Tests—Chi-square test, Spearman rank correlation, Mann-Whitney U tests, Bland-Altman analysis and receiver operating characteristic curve analysis.

Results—IER was higher for invasive cancer than for DCIS (R1/R2, $p<0.001$). IER increased with tumor grade (R1: $r=0.56$, $p<0.001$, R2: $r=0.50$, $p<0.001$), as ki-67 increased (R1: $r=0.35$, $p<0.001$; R2 $r=0.35$, $p<0.001$), and for node-positive disease (R1/R2, $p=0.001$). IER was higher

Corresponding Author: Laura Heacock, MD, Department of Radiology, New York University School of Medicine, 550 First Avenue, New York, New York, 10016, United States, (212) 263-3813, Fax: (212) 731-5554, Laura.Heacock@nyumc.org.

for human epidermal growth factor receptor two-positive and triple negative cancers than for estrogen receptor-positive/progesterone receptor-positive tumors (R1 p<0.001–0.002; R2 p=0.0.001–0.011). IER had higher sensitivity (80.6% vs 75.5%) and specificity (55.8% vs 48.1%) than washout curves for positive nodes, higher specificity (48.1% vs 36.5%) and positive predictive value (70.2% vs 66.7%) for high ki-67, and excellent inter-observer agreement (ICC=0.82).

Data Conclusion—IER, a measurement of early contrast wash-in, is associated with higher-grade malignancies and tumor aggressiveness and might be potentially incorporated into an AB-MRI protocol.

Keywords

breast MRI; temporal kinetics; breast cancer screening

INTRODUCTION

Dynamic contrast-enhanced (DCE) breast MRI has demonstrated high sensitivity for breast malignancies compared to screening breast ultrasound and mammography (1,2), and higher sensitivity and specificity than digital breast tomosynthesis (3,4). Although breast DCE-MRI is currently recommended only for screening high-risk women (5), it has been suggested as a more effective screening method for women at intermediate risk of breast cancer (6,7) and women with dense breast parenchyma (8,9). However, utilization of breast MRI remains limited by cost, availability, and interpretation time. A fast, abbreviated breast MRI (AB-MRI) screening exam with a 60–90 second scan time is therefore of recent interest (8,10–12), demonstrating high sensitivity for malignancy with short scan and interpretation times.

As most AB-MRI protocols are too short to evaluate wash-out curve analysis per Breast Imaging Reporting and Data System (BI-RADS) criteria (13), alternative and readily available measurements that incorporate wash-in temporal kinetic data could potentially add value in AB-MRI. Wash-in temporal kinetic data relies on the fast initial contrast uptake observed in high-grade DCIS and invasive cancers due to increased angiogenic activity (14–17). The added value of contrast wash-in is likely why MRI screening detects more biologically relevant high-grade DCIS and invasive cancers compared to other breast imaging modalities (18–21). Fast initial contrast wash-in has also been demonstrated in human epidermal growth factor receptor two-positive ($HER2^+$) and triple negative (TNBC) breast cancers (21), cancers with nodal metastases (22,23) and in tumors with high ki-67 (21), a marker of cell division and proliferation. As these factors independently predict more aggressive tumors that have lower disease-free and recurrence-free survival (24–27), evaluating markers of contrast wash-in in AB-MRI can offer important prognostic information.

Prior AB-MRI studies have evaluated the sensitivity and specificity of various protocols (8,10–12) and semi-quantitative parameters in sequences with temporal resolution of 10–20 seconds (28–31). Recent MRI sequences utilizing less than 10 seconds per frame (31,32) including compressed sensing methods (33,34) have advanced the possibility of high spatial and temporal resolution sequences allowing simultaneous morphological and semi-

quantitative analysis, but remain under development. Although highly sensitive for malignancy, the post-processing and increased turnaround time needed for deriving these semi-quantitative values are clinically impractical at present for most radiologists performing and interpreting breast MRI.

While most markers of initial contrast uptake are difficult to obtain with a temporal resolution greater than 20 seconds, one marker, the initial enhancement ratio (IER) (35), is easily measured on conventional DCE-MRI and has been shown in prior evaluation of AB-MRI to correlate to tumor grade (12). However, other wash-in features predicting tumor aggressiveness such as axillary nodal metastasis and biomarker expression have not been previously evaluated in the context of AB-MRI. As screening MRI preferentially detects biologically relevant cancer compared to mammography (18), retaining this ability in AB-MRI is of clinical importance. The purpose of our study was therefore to evaluate the feasibility of using IER, a measurement of contrast wash-in, as a surrogate marker for tumor grade, tumor receptor expression and aggressiveness in invasive ductal carcinoma and ductal carcinoma in situ (DCIS).

MATERIALS AND METHODS

Study Population

This Health Insurance Portability and Accountability (HIPAA)-compliant retrospective study was performed with approval from our Institutional Review Board (IRB) with waiver of informed consent. One hundred and sixty-two women (mean age 55.0, range 32.8–87.7 years) with one hundred and eighty-seven biopsy-proven malignancies were imaged between January 2012 and November 2015. Eighteen additional women imaged during this time underwent neoadjuvant chemotherapy prior to breast MRI and were excluded. The final cohort of 162 women had surgical pathology available for all lesions. Although all women underwent breast MRI for evaluation of extent of disease, at our institution a large percentage of these studies are TNBC and $HER2^{+}$ positive tumors due to the aggressiveness of these subtypes.

MR Imaging Technique

All women underwent bilateral breast DCE-MRI on a 3.0 T magnet (TimTrio, Siemens Medical Solutions, Erlangen, Germany) in the prone position using a dedicated surface breast coil (7-Channel Breast Biopsy Array, InVivo Research). The diagnostic protocol at our institution consisted of sagittal T1-weighted gradient echo, sagittal T2-weighted, sagittal T1-weighted gradient echo fat suppressed volume interpolated breath-hold exam (VIBE) pre- and three post contrast acquisitions beginning 70 seconds post-injection f Gd-DTPA (Magnevist, Bayer Healthcare, Leverkusen, Germany) at 0.1 mM/kg body weight at 2 mL/s via intravenous catheter followed by saline flush. Each VIBE acquisition time was 100 seconds with a total imaging time of 35 minutes. T1-weighted imaging parameters included: TR/TE = 4.01/1.52 msec, flip angle 12°, slice thickness 1 mm, matrix 384 × 384, FOV 270 mm. Subtraction images were automatically generated at the workstation by subtraction of the pre-contrast images from the first post-contrast images on a pixel by pixel basis. For the purposes of this study, a theoretical retrospective abbreviated MRI exam was used. It

consists of three sequences: the pre-contrast VIBE (100 seconds), first post-contrast VIBE (100 seconds) and corresponding automatically generated first post-contrast subtraction images. Since a localizer sequence (60 seconds) is performed prior to scanning the patient, the total imaging time for this abbreviated exam is four minutes and 20 seconds.

Pre- and post-contrast VIBE DCE-MRI images were transferred to a clinical workstation for post-processing by commercially available computer-aided detection (CAD) software (DynaCAD, Invivo, Gainesville, FL). This software automatically performs motion correction and generates conventional kinetic curve types based on pixel signal intensity compared between pre-contrast and post-contrast images.

Data Collection

First post-contrast images acquired at 70 seconds post-injection were used for lesion analysis. The previously described commercially available software (DynaCAD, Invivo, Gainesville, FL) was used to measure the initial enhancement ratio (IER; % signal increase over baseline at first post-contrast acquisition. IER was evaluated by two independent readers blinded to lesion pathology (A.A.L. and L.H., 3 years and 1 year experience each) by analyzing signal intensity changes in representative voxels on first post-contrast subtraction images. Readers used the CAD software to select a whole lesion ROI on a reader-selected slice of interest on first post-contrast subtraction images, excluding regions of necrosis and manually editing the ROI if necessary. The software then automatically selected the voxel with the highest percentage increase in signal intensity within that ROI (Figure 1). This value was recorded as the IER as previously described (12,35). The IER was compared with the conventional washout curves automatically generated by the same software for that lesion. If lesions demonstrated mixed curve types then the worst curve was recorded.

Contralateral and peritumoral background parenchymal enhancement (BPE) were assessed qualitatively on the first post-contrast subtraction image by a single reader (L.H., 1 year experience). Peritumoral BPE background parenchymal enhancement (BPE) was defined as the qualitative BPE measured within 5 mm from the tumor margin as previously described (36). BPE was graded on a 1–4 scale (minimal, mild, moderate and marked) corresponding to MRI BI-RADS criteria (13).

Medical records were reviewed for clinical-pathological data including size, tumor receptor expression (estrogen receptor (ER), progesterone receptor (PR) and HER2 positivity, ki-67, pathology-proven axillary metastases, Oncotype DX score (Genomic Health, Redwood City, CA), and tumor stage. ER/PR status was considered positive if 1% or more of the tumor cells showed nuclear staining at immunohistochemistry analysis as per American Society of Clinical Oncology/College of American Pathologists criteria. HER2 status was considered positive if immunohistochemistry result was 3+ (positive) or 2+ (borderline) confirmed by fluorescence in situ hybridization testing. Ki-67 was recorded as a scale measurement from 1–100% and considered high if greater than 14% (37). Oncotype DX is a 21-gene, breast-cancer specific expression profile used by clinicians to evaluate the likelihood of developing distant recurrence in ER-positive early stage breast cancer; results are used to determine the need for adjuvant chemotherapy. The Oncotype DX score can be stratified in three risk

categories: low (<18), intermediate (18–30) and high (>30) (38). Tumor grade, hormone receptor expression, presence of nodal metastases by needle biopsy or at time of surgery and high ki-67 have all been associated with rapid local spread, decreased time to recurrence, and decreased disease-free survival (24–27).

Statistical Analysis

Associations involving nominal categorical factors were assessed using the chi-square test. Bivariate associations of IER were assessed using the Spearman rank correlation. Subject groups defined in terms of specific features were compared in terms of IER from each reader using a Mann-Whitney test. Reader agreement in terms of IER was assessed using the concordance and intra-class correlation coefficients and the mean additive bias and limits of agreement from a Bland-Altman analysis. The utility of the IER values from both readers combined for the detection of specific binary features was assessed using a receiver operator characteristic (ROC) curve analysis with the Youden index as the criterion for identifying a threshold value of IER that maximized sensitivity and specificity of detection of that feature (39). The ROC analysis used the combined data from both readers in order to identify a reader-independent threshold (i.e., a single value that could be applied to the data from both readers for the purpose of classifying tumors as test positive or test negative for the feature).

Accuracy, sensitivity, specificity, positive predictive value (PPV) and negative predictive value (NPV) of IER were then compared to washout kinetic curves (type 3) (14) in the evaluation of invasive versus noninvasive cancer, biologically relevant disease (defined as high-grade DCIS and invasive cancers) versus more indolent disease, cancers with positive axillary nodes (with positive biopsy or pathology-proven at time of surgery) and cancers with high ki-67 (>14%) at pre-operative biopsy. Finally, the area under (AUC) the ROC curve was used to compare the diagnostic utility of IER and type 3 kinetic curves for these four outcomes using the Delong test. Differences in all statistical tests were conducted at the two-sided 5% significance level using SAS 9.4 (SAS Institute, Cary, NC).

RESULTS

Patient Population

The majority of patients (85.8%; 139/162) underwent MRI for extent of disease evaluation, with the remaining 14.1% (23/162) presenting for high-risk screening. Of 83 women with estrogen receptor-positive/progesterone receptor-positive (ER^+/PR^+) tumors, 48.2% (40/83) had Oncotype DX results available.

Lesion Pathology, Subtypes And Tumor Markers

Average lesion size was 2.44 cm (range 0.4–14 cm). Cancers were 73.3% (137/187) invasive ductal carcinoma (IDC), 4.8% (9/187) invasive lobular carcinoma (ILC) and 22.0% (41/187) ductal carcinoma in situ (DCIS). For invasive cancers, 19.2% (28/146) were triple negative breast cancers (TBNC) and 21.2% (31/146) were $HER2^+$ (Table 1). The majority of lesions were intermediate or high-grade invasive cancers (Table 2). Of 178 cases with final surgical nodal pathology, 27.5% (49/178) had pathology-proven nodes (by biopsy or at surgical

excision). Of the 151 invasive cancers with ki-67 available, 58.2% (88/151) had a ki-67 greater than 14%.

Correlation Of IER With Tumor Grades And Markers

Overall, IER was significantly higher in invasive cancer than in DCIS (both readers, $p<0.001$), and higher for invasive cancers and high-grade DCIS when compared to low and intermediate grade DCIS (both readers, $p<0.001$; Figure 2). IER showed a moderate and significant tendency to increase as tumor grade increased for all lesions (R1: $r=0.56$, $p<0.001$, R2: $r=0.50$, $p<0.001$; Figure 3). IER increased as lesion size (R1 $r=0.31$, $p<0.001$; R2 $r=0.28$, $p<0.001$) and ki-67 increased (R1: $r=0.35$, $p<0.001$; R2 $r=0.35$, $p<0.001$).

When correlated with tumor markers, mean IER was higher for $HER2^+$ (214.9% ± 68.7%, $p=0.002$) and TNBC (232.1% ± 75.3%, $p<0.001$) than for ER^+/PR^+ invasive cancers (167.6% ± 58.1%) for reader 1, and higher for $HER2^+$ (226.8% ± 66.0%, $p=0.011$) and TNBC (237.7% ± 56.0%, $p=0.001$) than for ER^+/PR^+ cancers (190.4% ± 70.1%) for reader 2. There was no difference between mean IER of $HER2^+$ and TNBC for either reader ($p=0.366–0.439$). Mean IER was higher for invasive cancers with positive nodes (R1: 213.0% ± 72.2%, R2: 233.4% ± 68.3%) than for negative nodes (R1: 158.8% ± 66.9%, R2: 173.2% ± 72.7%, $p<0.001$ for both readers) at surgical resection. There was no correlation between IER and Oncotype DX score (R1 $p=0.139$, R2 $p=0.136$) for ER^+/PR^+ tumors.

IER Diagnostic Utility, Sensitivity, Specificity, PPV And NPV

The area under the curve of a ROC curve analysis was used to pick a threshold IER maximizing the sum of sensitivity and specificity (i.e., Youden index) (31). IER AUC was significant for each of the four tested clinical factors: biopsy-proven metastatic axillary nodes (AUC 0.720), invasive cancer (AUC 0.798), biologically relevant cancer (AUC 0.797) and high ki-67 (AUC 0.672, all $p<0.001$).

Compared to Type 3 washout curves, IER had higher sensitivity (80.6% vs 76.5%) and specificity (55.8% vs 48.1%) for positive axillary nodes but was less sensitive (59.9% vs 73.3%) and specific (85.4% vs 87.8%) for invasive cancers. IER was less sensitive (60.9% vs 64.7%) but equally specific (88.2%) for biologically relevant cancers, and less sensitive (78.4% vs 81.5%) for high ki-67 but more specific (48.1% vs 36.5%). IER had higher PPV than Type 3 curves for positive nodes (40.9% vs 35.6%) and high ki-67 (70.2% vs 66.7%) (Table 4).

When using the area under the curve as a measure of the overall diagnostic utility of IER, IER had higher AUC (0.720) than Type 3 curves (0.618) for positive axillary nodes, a statistically significant finding ($p=0.004$). There was no significant difference in the AUC for IER and Type 3 curves for invasive cancers ($p=0.813$), biologically relevant cancers ($p=0.440$) or high ki-67 ($p=0.073$) (Table 4). Lesion shape and internal enhancement pattern could not be compared between IER and washout curve types due to insufficient subgroup numbers.

IER And BPE

IER increased as contralateral BPE (r=0.24–0.29, p<0.001), ipsilateral BPE (r=0.25–0.31, p<0.001) and peritumoral BPE increased (R1 r=0.26 p<0.001; R2 r=0.22, p=0.003). However, there was no correlation between BPE and size (p=0.054–0.202), tumor grade (p=0.435–0.958), ki-67 (p=0.234–0.691) or axillary node status at final excision (p=0.890, p=0.129).

IER And Reader Agreement

There was substantial inter-observer agreement for IER measurements, with both concordance and intra-class correlation coefficients of 0.82. No significant trend was seen on Bland-Altman analysis (Figure 4).

DISCUSSION

In this study we evaluated the IER as a marker of early contrast wash-in and found a moderate, significant correlation between tumor grade and IER, with increased IER in high grade DCIS and invasive cancers. The correlation of IER with tumor grade likely reflects the increased angiogenesis seen in these lesions, leading to faster wash-in of contrast (14–16,21). Although the association of wash-in temporal kinetics and tumor grade has been examined previously in full diagnostic protocols, it has not been extensively studied in a conventional AB-MRI with temporal resolution of 2–3 minutes. Our results are similar to that of Heacock et al, who found a similar moderate correlation between IER and tumor grade in AB-MRI (12). Notably, higher IER in that study also increased AB-MRI lesion conspicuity and reader confidence in diagnosis.

IER was also increased in $HER2^+$ and TNBC when compared to ER+/PR+ breast cancers. $HER2^+$ and TNBC cancers are diagnosed at later stages, grow more quickly and have a higher chance of recurrence and higher mortality rate than ER^+/PR^+ cancers (25,26). As both $HER2^+$ and TNBC cancers are more likely to require neoadjuvant chemotherapy prior to surgery (25,26), identifying these receptor subtypes at the time of screening MRI would allow for earlier oncology referral and initiation of treatment. IER in our study also correlated with high ki-67, a marker of cell proliferation, and with node-positive invasive cancers. Similar to $HER2^+$ and TNBC, high ki-67 and positive axillary nodes at time of diagnosis are associated with rapid local spread, decreased time to recurrence, and decreased disease-free survival (24,27). As high IER parallels the presence of these prognostic indicators, identifying cancers with higher IER can potentially identify more aggressive breast cancers.

The majority of studies to date of temporal kinetics in AB-MRI have focused on sequences with a temporal resolution of less than 10–20 seconds. These studies have demonstrated that malignant lesions have early arterial enhancement that occurs prior to background parenchymal enhancement in early post-contrast imaging. Mann et al found that maximum slope could distinguish benign from malignant lesions at 60 seconds with a sensitivity of 90% and specificity of 67% (30). Pineda et al similarly demonstrated that the initial slope for malignant lesions was at least six times that of benign lesions at 60 second post-injection

(32). Tudorica et al demonstrated that semi-quantitative parameters derived from a 60 second acquisition have 100% sensitivity and 91% specificity (31). No studies to date have evaluated the utility of the parameters derived from these novel sequences to differentiate tumor grade, receptor status, or similar markers of prognosis. Although these sequences offer high sensitivity for contrast wash-in, many trade increased temporal resolution for decreased spatial resolution and are not yet clinically practical for radiologists interpreting breast MRI. The chief advantage of IER compared to these measurements is that it can be quickly incorporated into current clinical use using conventional post-processing software without requiring advanced imaging sequences or off-line reconstruction. The strong inter-observer agreement in our study furthermore suggests the high reproducibility of this measurement.

In our study we also compared the diagnostic utility of IER to the gold-standard of wash-out kinetic curves and found that IER offers higher diagnostic utility for positive axillary nodes, with similar diagnostic utility to wash-out curves for biologically relevant cancers, invasive cancers, high ki-67 and positive axillary nodes. IER also offers higher specificity and positive predictive value for lesions with high ki-67. As wash-out curves cannot be used by definition in AB-MRI (13), the similar diagnostic utility of IER suggests it is a reasonable alternative to washout curves in AB-MRI.

Although IER predicted tumor grade and receptor status and increased with higher background parenchymal enhancement, there was no such correlation with BPE or peritumoral BPE and tumor grade, size, axillary status or ki-67. This finding suggests that IER reflects tumor angiogenesis rather than simply paralleling BPE. The correlation of IER but not BPE to tumor grade may also reflect our use of the first post-contrast scan to evaluate BPE, which enhances more slowly over time than most cancers and is higher at delayed time points (40).

Limitations of our study include its small sample size and its retrospective nature. Although higher numbers of DCIS and invasive cancer tumor grades would be optimal, pure low-grade DCIS and low-grade $HER2^+$ and TNBC invasive cancers are less frequent in our population as reflected in the general population (25,26). We also did not evaluate the ability of IER to discriminate between benign and malignant tumors. As this was intended as a proof-of-concept study to evaluate the feasibility of including IER measurements in an AB-MRI, we chose to initially test this measurement in a population of known cancers. Further investigation of the use of IER prospectively in an AB-MRI in a larger screening population is ongoing and will allow us to evaluate both sensitivity and specificity in the context of AB-MRI.

In conclusion, high IER at first post-contrast imaging may be a useful imaging biomarker for higher-grade malignancy, $HER2^+$ and TNBC cancers, and axillary invasion, all of which are associated with of tumor recurrence after therapy. The high specificity and PPV of IER compared to wash-out curves suggest use of this measurement may also help decrease recalls and false-positive biopsies. As clinical interest grows in an abbreviated breast MRI protocol for screening, temporal kinetic measurements that can be incorporated into current workflows with conventional equipment are of increasing importance. IER is associated with

higher-grade malignancies and tumor aggressiveness that is both easily assessed and integrated into an abbreviated breast MRI protocol.

Acknowledgments

Grant Support: NIH R01CA160620 (S.G.K.).

References

1. Berg WA, Zhang Z, Lehrer D, et al. Detection of breast cancer with addition of annual screening ultrasound or a single screening MRI to mammography in women with elevated breast cancer risk. Jama. 2012; 307(13):1394–1404. [PubMed: 22474203]
2. Kuhl C, Weigel S, Schrading S, et al. Prospective multicenter cohort study to refine management recommendations for women at elevated familial risk of breast cancer: the EVA trial. Journal of clinical oncology : official journal of the American Society of Clinical Oncology. 2010; 28(9):1450–1457. [PubMed: 20177029]
3. Wallis MG, Moa E, Zanca F, Leifland K, Danielsson M. Two-view and single-view tomosynthesis versus full-field digital mammography: high-resolution X-ray imaging observer study. Radiology. 2012; 262(3):788–796. [PubMed: 22274840]
4. Rafferty EA, Park JM, Philpotts LE, et al. Assessing radiologist performance using combined digital mammography and breast tomosynthesis compared with digital mammography alone: results of a multicenter, multireader trial. Radiology. 2013; 266(1):104–113. [PubMed: 23169790]
5. Lee CH, Dershaw DD, Kopans D, et al. Breast cancer screening with imaging: recommendations from the Society of Breast Imaging and the ACR on the use of mammography, breast MRI, breast ultrasound, and other technologies for the detection of clinically occult breast cancer. Journal of the American College of Radiology : JACR. 2010; 7(1):18–27. [PubMed: 20129267]
6. Brennan S, Liberman L, Dershaw DD, Morris E. Breast MRI screening of women with a personal history of breast cancer. AJR American journal of roentgenology. 2010; 195(2):510–516. [PubMed: 20651211]
7. Sung JS, Malak SF, Bajaj P, Alis R, Dershaw DD, Morris EA. Screening breast MR imaging in women with a history of lobular carcinoma in situ. Radiology. 2011; 261(2):414–420. [PubMed: 21900617]
8. Kuhl CK, Schrading S, Strobel K, Schild HH, Hilgers RD, Bieling HB. Abbreviated breast magnetic resonance imaging (MRI): first postcontrast subtracted images and maximum-intensity projection-a novel approach to breast cancer screening with MRI. Journal of clinical oncology : official journal of the American Society of Clinical Oncology. 2014; 32(22):2304–2310. [PubMed: 24958821]
9. Kriege M, Brekelmans CT, Obdeijn IM, et al. Factors affecting sensitivity and specificity of screening mammography and MRI in women with an inherited risk for breast cancer. Breast cancer research and treatment. 2006; 100(1):109–119. [PubMed: 16791481]
10. Mango VL, Morris EA, David Dershaw D, et al. Abbreviated protocol for breast MRI: are multiple sequences needed for cancer detection? European journal of radiology. 2015; 84(1):65–70. [PubMed: 25454099]
11. Grimm LJ, Soo MS, Yoon S, Kim C, Ghate SV, Johnson KS. Abbreviated screening protocol for breast MRI: a feasibility study. Academic radiology. 2015; 22(9):1157–1162. [PubMed: 26152500]
12. Heacock L, Melsaether AN, Heller SL, et al. Evaluation of a known breast cancer using an abbreviated breast MRI protocol: Correlation of imaging characteristics and pathology with lesion detection and conspicuity. European journal of radiology. 2016; 85(4):815–823. [PubMed: 26971429]
13. Morris, EACC., Lee, CH. ACR BI-RADS® Atlas, Breast Imaging Reporting and Data System. Reston, VA: American College of Radiology; 2013. ACR BI-RADS® Magnetic Resonance Imaging.

14. Kuhl CK, Schild HH, Morakkabati N. Dynamic bilateral contrast-enhanced MR imaging of the breast: trade-off between spatial and temporal resolution. Radiology. 2005; 236(3):789–800. [PubMed: 16118161]
15. Rahbar H, Partridge SC, Demartini WB, et al. In vivo assessment of ductal carcinoma in situ grade: a model incorporating dynamic contrast-enhanced and diffusion-weighted breast MR imaging parameters. Radiology. 2012; 263(2):374–382. [PubMed: 22517955]
16. Sardanelli F, Rescinito G, Giordano GD, Calabrese M, Parodi RC. MR dynamic enhancement of breast lesions: high temporal resolution during the first-minute versus eight-minute study. Journal of computer assisted tomography. 2000; 24(5):724–731. [PubMed: 11045693]
17. Schabel MC, Morrell GR, Oh KY, Walczak CA, Barlow RB, Neumayer LA. Pharmacokinetic mapping for lesion classification in dynamic breast MRI. Journal of magnetic resonance imaging : JMRI. 2010; 31(6):1371–1378. [PubMed: 20512889]
18. Sung JS, Stamler S, Brooks J, et al. Breast Cancers Detected at Screening MR Imaging and Mammography in Patients at High Risk: Method of Detection Reflects Tumor Histopathologic Results. Radiology. 2016; 280(3):716–722. [PubMed: 27097237]
19. Buadu LD, Murakami J, Murayama S, et al. Breast lesions: correlation of contrast medium enhancement patterns on MR images with histopathologic findings and tumor angiogenesis. Radiology. 1996; 200(3):639–649. [PubMed: 8756909]
20. Leong LC, Gombos EC, Jagadeesan J, Fook-Chong SM. MRI kinetics with volumetric analysis in correlation with hormonal receptor subtypes and histologic grade of invasive breast cancers. AJR American journal of roentgenology. 2015; 204(3):W348–356. [PubMed: 25714321]
21. Szabo BK, Aspelin P, Kristoffersen Wiberg M, Tot T, Bone B. Invasive breast cancer: correlation of dynamic MR features with prognostic factors. European radiology. 2003; 13(11):2425–2435. [PubMed: 12898176]
22. Mussurakis S, Buckley DL, Horsman A. Dynamic MR imaging of invasive breast cancer: correlation with tumour grade and other histological factors. The British journal of radiology. 1997; 70(833):446–451. [PubMed: 9227224]
23. Tuncbilek N, Karakas HM, Okten OO. Dynamic magnetic resonance imaging in determining histopathological prognostic factors of invasive breast cancers. European journal of radiology. 2005; 53(2):199–205. [PubMed: 15664283]
24. Azambuja E, Cardoso F, Castro G, et al. Ki-67/MIB-1 as prognostic marker in women with early breast cancer: a meta-analysis of published studies involving 10. 958 patients. Breast cancer research and treatment. 2005; 94:S127–S127.
25. Curigliano G, Viale G, Bagnardi V, et al. Clinical relevance of HER2 overexpression/amplification in patients with small tumor size and node-negative breast cancer. Journal of clinical oncology : official journal of the American Society of Clinical Oncology. 2009; 27(34):5693–5699. [PubMed: 19884553]
26. Haffty BG, Yang Q, Reiss M, et al. Locoregional relapse and distant metastasis in conservatively managed triple negative early-stage breast cancer. Journal of clinical oncology : official journal of the American Society of Clinical Oncology. 2006; 24(36):5652–5657. [PubMed: 17116942]
27. Jatoi I, Hilsenbeck SG, Clark GM, Osborne CK. Significance of axillary lymph node metastasis in primary breast cancer. Journal of clinical oncology : official journal of the American Society of Clinical Oncology. 1999; 17(8):2334–2340. [PubMed: 10561295]
28. Abe, H., Mori, N., Tsuchiya, K., et al. AJR American journal of roentgenology. 2016. Kinetic Analysis of Benign and Malignant Breast Lesions With Ultrafast Dynamic Contrast-Enhanced MRI: Comparison With Standard Kinetic Assessment; p. 1-8.
29. Pineda FD, Medved M, Wang S, et al. Ultrafast Bilateral DCE-MRI of the Breast with Conventional Fourier Sampling: Preliminary Evaluation of Semi-quantitative Analysis. Academic radiology. 2016; 23(9):1137–1144. [PubMed: 27283068]
30. Mann RM, Mus RD, van Zelst J, Geppert C, Karssemeijer N, Platel B. A novel approach to contrast-enhanced breast magnetic resonance imaging for screening: high-resolution ultrafast dynamic imaging. Investigative radiology. 2014; 49(9):579–585. [PubMed: 24691143]

31. Tudorica LA, Oh KY, Roy N, et al. A feasible high spatiotemporal resolution breast DCE-MRI protocol for clinical settings. Magnetic resonance imaging. 2012; 30(9):1257–1267. [PubMed: 22770687]
32. Pineda FD, Medved M, Wang S, et al. Ultrafast Bilateral DCE-MRI of the Breast with Conventional Fourier Sampling: Preliminary Evaluation of Semi-quantitative Analysis. Academic radiology. 2016
33. Kim SG, Feng L, Grimm R, et al. Influence of temporal regularization and radial undersampling factor on compressed sensing reconstruction in dynamic contrast enhanced MRI of the breast. Journal of magnetic resonance imaging : JMRI. 2016; 43(1):261–269. [PubMed: 26032976]
34. Heacock L, Gao Y, Heller SL, et al. Comparison of conventional DCE-MRI and a novel golden-angle radial multicoil compressed sensing method for the evaluation of breast lesion conspicuity. Journal of magnetic resonance imaging : JMRI. 2016
35. Heller SL, Moy L, Lavianlivi S, Moccaldi M, Kim S. Differentiation of malignant and benign breast lesions using magnetization transfer imaging and dynamic contrast-enhanced MRI. Journal of magnetic resonance imaging : JMRI. 2013; 37(1):138–145. [PubMed: 23097239]
36. Kim SA, Cho N, Ryu EB, et al. Background parenchymal signal enhancement ratio at preoperative MR imaging: association with subsequent local recurrence in patients with ductal carcinoma in situ after breast conservation surgery. Radiology. 2014; 270(3):699–707. [PubMed: 24126372]
37. Goldhirsch A, Wood WC, Coates AS, et al. Strategies for subtypes-dealing with the diversity of breast cancer: highlights of the St Gallen International Expert Consensus on the Primary Therapy of Early Breast Cancer 2011. Ann Oncol. 2011; 22(8):1736–1747. [PubMed: 21709140]
38. Paik S, Tang G, Shak S, et al. Gene expression and benefit of chemotherapy in women with node-negative, estrogen receptor-positive breast cancer. Journal of Clinical Oncology. 2006; 24(23): 3726–3734. [PubMed: 16720680]
39. Youden WJ. Index for rating diagnostic tests. Cancer. 1950; 3(1):32–35. [PubMed: 15405679]
40. Melsaether A, Pujara AC, Elias K, et al. Background parenchymal enhancement over exam time in patients with and without breast cancer. Journal of magnetic resonance imaging : JMRI. 2016

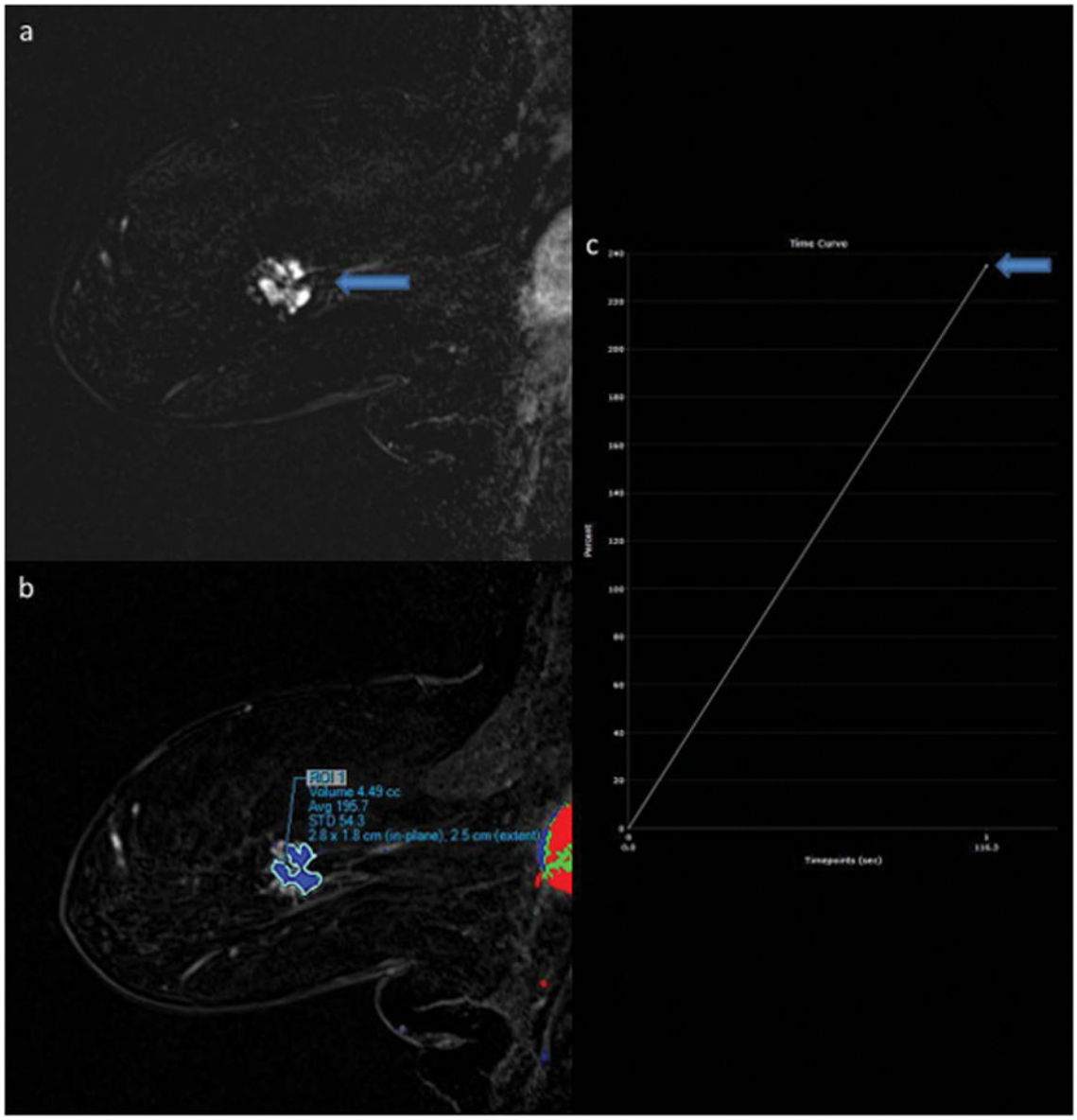

Figure 1.

88-year-old woman presenting with new diagnosis of right breast cancer. A 3.2 cm breast mass is seen the posterior left breast on the sagittal T1-weighted post-contrast subtraction image (1A, arrow) on first post-contrast images. Lesion ROI (1B) demonstrated IER of 235% when measured by Reader 1 (1C, arrow) and 248% by Reader 2 on first post-contrast images. MR-guided biopsy yielded intermediate-grade invasive ductal carcinoma.

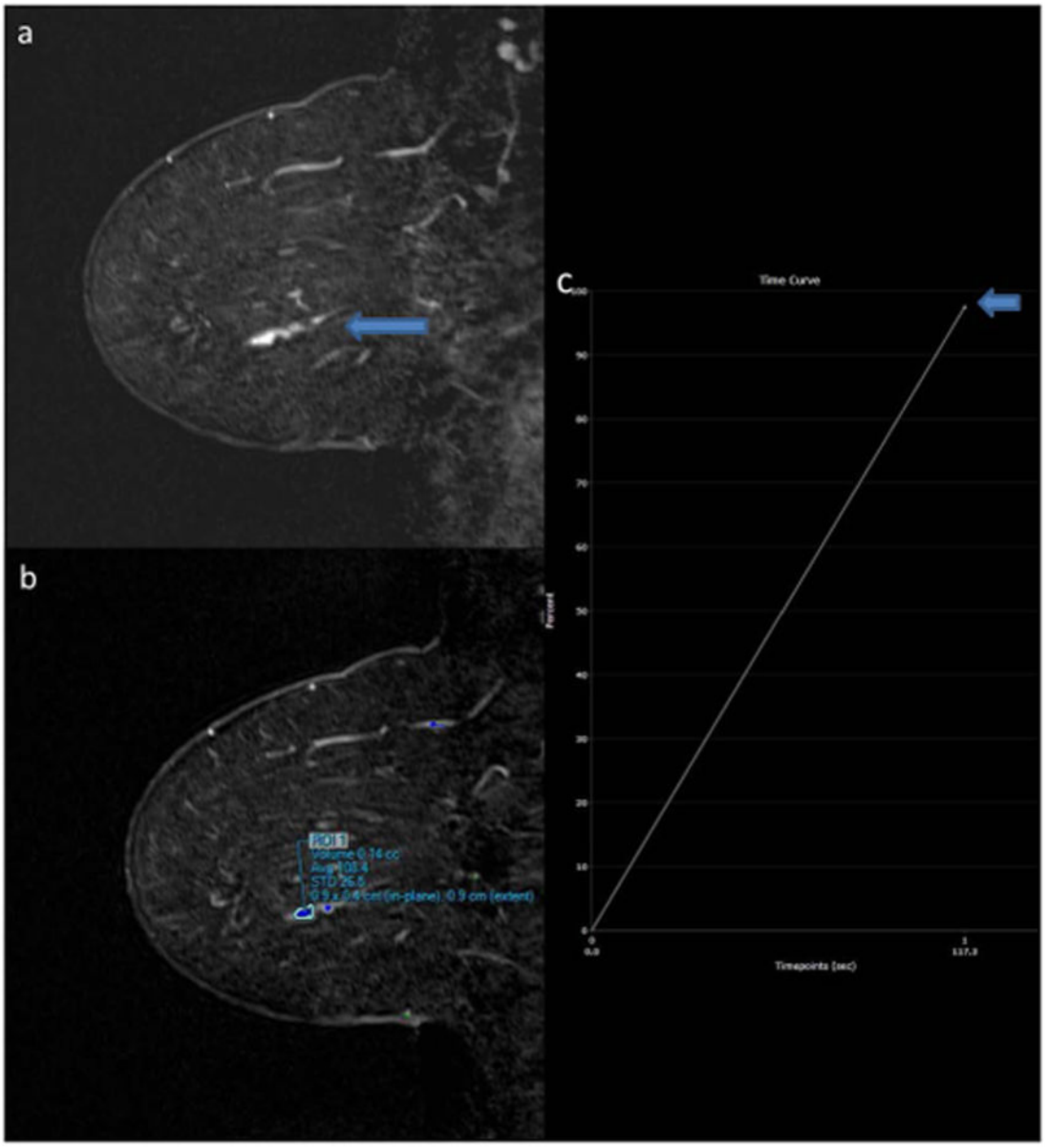

Figure 2.

58-year-old woman with history of bilateral papillomas status post surgical excision. New 2.0 cm linear clumped nonmass enhancement is present on the sagittal T1-weighted post-contrast subtraction image of the left breast on surveillance MRI (2A, arrow). Lesion ROI (2B) demonstrated IER of 98% when measured by Reader 1 (2C, arrow) and 72% by Reader 2 on first post-contrast images. MR-guided biopsy yielded intermediate-grade ductal carcinoma in situ.

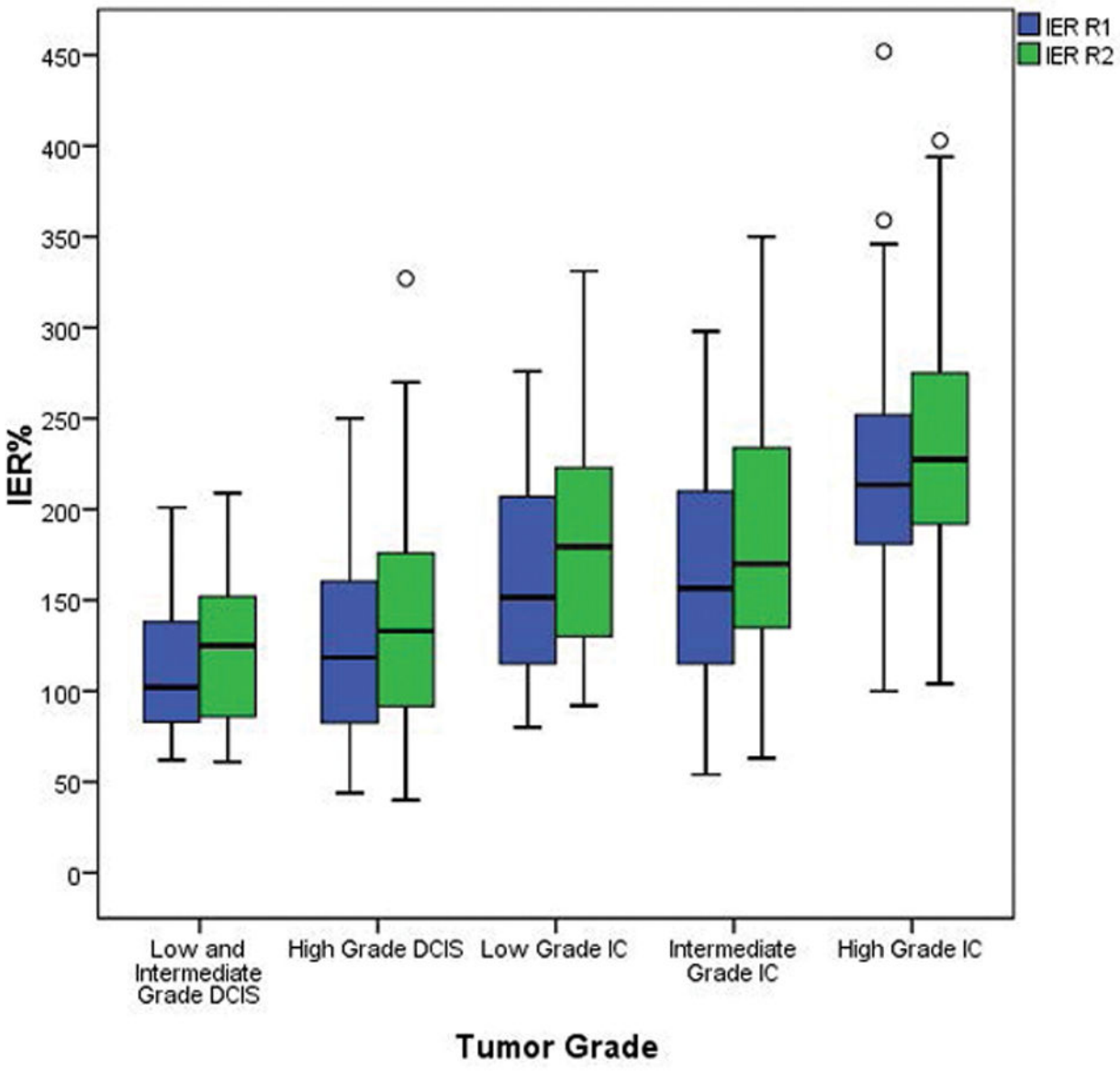

Figure 3.

Median initial enhancement ratio (IER; % enhancement over baseline on first post-contrast images) of breast lesions by tumor grade. There was a moderate but significant tendency of IER to increase as tumor grade increased (R1: r=0.56, p<0.001, R2: r=0.50, p<0.001). DCIS = ductal carcinoma in situ. IC = invasive carcinoma.

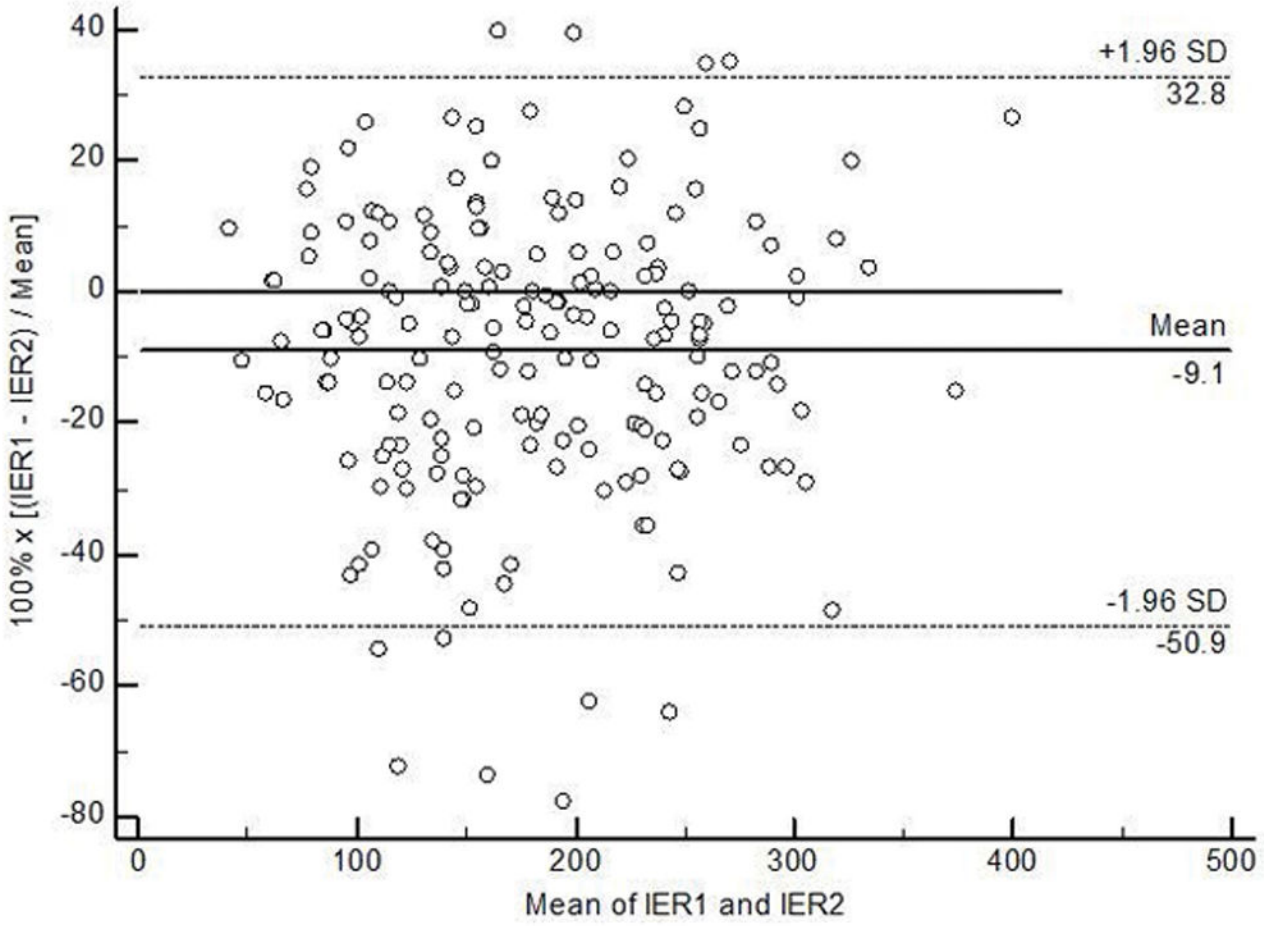

Figure 4.
Bland-Altman plot to assess agreement of IER measurements between readers. Intraclass correlation coefficient and concordance correlation coefficient were both 0.82.

Table 1

ER^+/PR^+, TNBC and $HER2^+$ invasive cancers by tumor grade at final pathology. ER^+/PR^+= estrogen receptor-positive/progesterone receptor-positive, TNBC= triple negative breast cancer, $HER2^+$ = human epidermal growth factor receptor two-positive.

	ER^+/PR^+ (n=83)	TNBC (n=28)	$HER2^+$ (n=31)
Low grade	31.3% (26/83)	0.0% (0/28)	0.0% (0/31)
Intermediate grade *	51.8% (43/83)	0.0% (0/28)	19.4% (6/31)
High grade *	16.9% (14/83)	100.0% (28/28)	80.6% (25/31)

* One intermediate and three high grade invasive cancers (4/146) had incomplete tumor markers.

Table 2

Pathology grade and stage for all cancers. IDC= invasive ductal carcinoma. ILC = invasive lobular carcinoma. DCIS = ductal carcinoma in situ.

Type	**N = 187**
Invasive Carcinoma	146/187 (78.0%)
IDC	137/187 (73.3%)
Low grade	26/137 (18.9%)
Intermediate grade	50/137 (36.5%)
High grade	70/137 (51.1%)
ILC	9/187 (4.8%)
Low grade	0/9 (0.0%)
Intermediate grade	6/9 (66.7%)
High grade	3/9 (33.3%)
Carcinoma in Situ	
DCIS	41/187 (21.9%)
Low grade	2/41 (4.9%)
Intermediate grade	15/41 (36.6%)
High grade	24/41 (58.5%)
Stage at diagnosis	N = 162
0 (in situ)	32/162 (19.8%)
IA	69/162 (42.6%)
IB	2/162 (1.2%
IIA	25/162 (15.4%)
IIB	7/162 (4.3%)
IIIA	15/162 (9.3%)
IIIB	2/162 (1.2%)
IIIC	2/162 (1.2%)
IV	6/162 (3.7%)
Final staging unavailable	2/162 (1.2%)

Table 3

The overall sensitivity, specificity, positive predictive value (PPV), negative predictive value (NPV) and area under the curve (AUC) of the initial enhancement ratio (IER) compared to washout (type 3) curves. For each component of diagnostic accuracy, the denominators for IER are larger than the corresponding denominators for curve since IER values were provided for each patient by two independent readers.

Outcome	Measure	IER	Type 3 Curve	P-value
Positive axillary nodes	Specificity	55.8% (144/258)	48.1% (62/129)	
	Sensitivity	80.6% (79/98)	75.5% (37/49)	
	NPV	88.3% (144/163)	83.8% (62/74)	
	PPV	40.9% (79/193)	35.6% (37/104)	
	AUC	0.720	0.618	**0.004**
Invasive cancer	Specificity	85.4% (70/82)	87.8% (36/41)	
	Sensitivity	59.9% (175/292)	73.3% (107/146)	
	NPV	37.4% (70/187)	48.0% (36/75)	
	PPV	93.6% (175/187)	95.5% (107/112)	
	AUC	0.798	0.805	0.813
Biologically relevant cancers	Specificity	88.2% (30/34)	88.2% (15/17)	
	Sensitivity	60.9% (207/340)	64.7% (110/170)	
	NPV	18.4% (30/163)	20.0% (15/75)	
	PPV	98.1% (207/211)	98.2% (110/112)	
	AUC	0.797	0.765	0.440
Ki-67 > 14%	Specificity	48.1% (50/104)	36.5% (19/52)	
	Sensitivity	78.4% (127/162)	81.5% (66/81)	
	NPV	58.8% (50/85)	55.9% (19/34)	
	PPV	70.2% (127/181)	66.7% (66/99)	
	AUC	0.672	0.590	0.073